Interdependence of Conformational Variables in Double-Helical DNA

A. Sarai,* R. L. Jernigan,# and J. Mazur§
*RIKEN Life Science Center, Tsukuba, Ibaraki 305, Japan; #Laboratory of Mathematical Biology, DBS, National Cancer Institute, National Institutes of Health, Bethesda, Maryland 20892-5677 USA; and §Frederick Biomedical Super Computing Laboratory, SAIC, NCI-FCRDC, Frederick, Maryland 21701 USA

ABSTRACT DNA exhibits conformational polymorphism, with the details depending on the sequence and its environment. To understand the mechanisms of conformational polymorphism and these transitions, we examine the interrelationships among the various conformational variables of DNA. In particular, we examine the stress-strain relation among conformational variables, describing base-pair morphology and their effects on the backbone conformation. For the calculation of base pairs, we use the method previously developed to calculate averages over conformational variables of DNA. Here we apply this method to calculate the Boltzmann averages of conformational variables for fixed values of one particular conformational variable, which reflects the strain in the structure responding to a particular driving stress. This averaging over all but one driving variable smooths the usual rough energy surface to permit observation of the effects of one conformational variable at a time. The stress-strain analyses of conformational variables of base pair slide, twist, and roll, which exhibit characteristic changes during the conformational transition of DNA, have shown that the conformational changes of base pairs are strongly correlated with one another. Furthermore, the stress-strain relations are not symmetrical with respect to these variables, i.e., the response of one coordinate to another is different from the reverse direction. We also examine the effect of conformational changes in base-pair variables on the sugar-backbone conformation by using the minimization method we developed. The conformational changes of base pairs affect the sugar pucker and other dihedral angles of the backbone of DNA, but each variable affects the sugar-backbone differently. In particular, twist is found to have the most influence in affecting the sugar pucker and backbone conformation. These calculated conformational changes in base pairs and backbone segments are consistent with experimental observations and serve to validate the calculation method.

INTRODUCTION

Usually DNA exists in the B-form in solution, but some sequences, especially those with higher G/C content, convert to the A-form under low humidity or in ethanol solutions (Pilet and Brahms, 1972; Ivanov et al., 1973; Arnott and Selsing, 1974; Leslie et al., 1980), and alternating purine-pyrimidine sequences can convert to the Z-form in high-salt media (Pohl and Jovin, 1972). There are several important characteristics of the different forms of DNA, such as different sugar puckers, dihedral angles of the backbone, groove widths, and helical pitches (Saenger, 1984). These characteristics have been widely investigated by structural, spectroscopic, and theoretical analyses (Arnott and Hukins, 1972; Olson and Flory, 1972; Sasisekharan, 1973; Bloomfield et al., 1974; Levitt and Warshel, 1978; Dickerson and Drew, 1981; Shakked and Kennard, 1985; Sarma et al., 1986). However, detailed mechanisms of the conformational polymorphism and transitions among different conformations are not understood. In the case of A-form DNA, sugar pucker is C_3'-*endo*, whereas the B-form usually has C_2'-*endo* conformation. The A-form has different phosphate-sugar dihedral angles than the B-form, and the major groove is wider and deeper than the B-form. In terms of base-pair morphology, one of the most distinctive differences between the two forms is the slide along the long axis of the base pair; base pairs in the A-form are displaced by about -1.5 Å along the slide direction outward from the helix axis relative to the B-form. The A-form base pairs also have a smaller twist about the helical axis, with about 31° of twist angle compared to 36° in the B-form. The roll angle tends to be positive, which gives rise to a base inclination with respect to the global helix axis of DNA. What do these characteristics imply about the mechanism of the conformational transition between the A- and B-forms? It has been suggested that the difference in the hydration in the groove may be related to conformational preferences (Alden and Kim, 1979). Observation of a spine of ordered water molecules in the minor groove of a B-DNA crystal structure led to a suggestion that the change in the water structure may cause the B-A transition (Drew and Dickerson, 1981). It has also been suggested that the economy of hydration around phosphate groups may be important for the stabilization of A-form DNA (Saenger et al., 1986). Although these models point out factors that may affect the transition, it is not possible to tell whether these characteristics are the causes or the results of the transition. Conformational characteristics of B- and A-form DNA have been analyzed by computer simulations (Levitt and Warshel, 1978; Zhurkin et al., 1978; Kollman et al., 1982; Ulyanov and Zhurkin, 1984; Tung and Harvey, 1986; Srinivasan and Olson; 1987; Fritsch et al., 1993; Briki and Genet, 1994), which usually consider all atoms of DNA. Although such calculations can reveal conformational characteristics of

Received for publication 17 August 1995 and in final form 7 June 1996.
Address reprint requests to Dr. Robert Jernigan, Laboratory of Mathematical Biology, Bldg. 12B, Room B-116, DBS, National Cancer Institute, National Institutes of Health, Bethesda, MD 20892-5677. Tel.: 301-496-4783; Fax: 301-402-4724; E-mail: jernigan@lmmb.nci.nih.gov.

0006-3495/96/09/1507/12 $2.00

DNA, they tend to obscure the interrelationships among conformational variables. To understand the conformation polymorphism and the mechanisms of transitions, here we will analyze the detailed energetics of the transition process and the interrelation among conformation variables.

Previously we developed a method to calculate thermodynamic averages for the conformational variables of DNA (Sarai et al., 1988a,b; Mazur et al., 1989), by which we can estimate an adiabatic free energy profile along a particular coordinate. We have applied this method to the analyses of base-pair conformations without a backbone (Sarai et al., 1988b), to assess its flexibility (Sarai et al., 1989) and to examine the effect of sequence and environment on the tendency of DNA to be in either the B- or the A-form (Mazur et al., 1989). The method is also suited to examining the response of one conformational coordinate (strain) to changes in another coordinate (stress), because such an analysis for the microscopic system requires thermodynamic averaging. Here we examine by this method the stress-strain relationship among the various conformational variables of base pairs. For the backbone calculations, however, we cannot apply the same method, because the larger number of degrees of freedom would present computational difficulties. Thus, we investigate the backbone conformation by using a new energy minimization technique. To avoid the local-minimum problem, we have developed the minimization method presented in the preceding article. We combine the two kinds of calculations for base pairs and for sugar-phosphate backbones, to examine the stress-strain relationships among base-pair coordinates and their effects on the backbone conformation. These results will be compared with experimental observations on the B- and A-forms of DNA. Possible implications for conformational transitions will be discussed.

METHOD OF CALCULATION

Statistical calculations on base pairs not yet connected with backbones, and on backbones connected to structurally rigid bases, are performed separately and independently. For the calculation of the conformational free energy of base pairs, we generate large numbers of conformations to estimate the partition function. The details of our method of calculation were described previously (Sarai et al., 1988a,b; Mazur et al., 1989). The backbone calculations were detailed in the preceding paper. In either case, we follow the guideline of an EMBO workshop (Dickerson et al., 1989) for the definitions of the coordinate system to describe the relative orientation of two neighboring base pairs and their transformations. Both the coordinate system detailed in our previous works and the one established in the EMBO workshop conform with the right-handed orthogonal coordinate system. Therefore, they can be interchanged without changing their space directions. These considerations have significance when dealing with the backbone dihedral angles. A left-handed coordinate system (e.g., the system often employed before the EMBO convention) would not only result in the reversal of the signs of the calculated dihedral angles, but would also affect their magnitudes in the iterative algorithm, unless the direction of the energy minimization were also reversed. This happens because the sign of a dihedral angle is determined by a sign of a certain determinant formed by differences in the X, Y, and Z coordinates in the four-atom sets that define the dihedral angle. The sign of this determinant is invariant only if the same sequence of coordinates has been put through an even number of permutations of the X, Y, and Z coordinates.

The rotational orientation of the second base pair coordinate system ($X'Y'Z'$) with respect to the first coordinates (XYZ) can be uniquely specified in terms of the nine direction cosines of the transformation matrix between the two coordinate systems. In the present calculations, the rotational transformation is performed with three Euler angles, designated by Goldstein (1981) as the z convention. The rotation convention is designated by the second rotation. The conventional three angles, "twist," "roll," and "tilt," can be obtained directly from the nine direction cosines of a transformation matrix (Sarai et al., 1988a,b) based on these Euler angles.

Different electrostatic potentials of mean force are employed in calculations performed on an isolated base pair alone and for a backbone connected to structurally rigid bases. The motivation for this dual electrostatic model was detailed and explained in the preceding paper. For calculations of isolated base pairs alone, we use the following potential V_{es} (in kcal/mol) to take account of the dielectric damping effect between base pairs:

$$V_{es} = 332\sum_{ij}(1/\epsilon_0 r_{ij})C_iC_j \exp(-\alpha_0(r_{ij} - r_0)) \quad r_{ij} > r_0,$$
$$V_{es} = 332\sum_{ij}(1/\epsilon_0 r_{ij})C_iC_j \quad r_{ij} < r_0, \tag{1}$$

where α_0 is the ionic screening parameter in units of $Å^{-1}$ and ϵ_0 is the limiting value of dielectric constant at distances less than r_0; 332 is a constant to give energy in units of kcal/mol; C_i and C_j are partial atomic charges (from Zhurkin et al., 1981); r_0 represents a cavity size, within which the dielectric constant remains uniform; and ϵ_{eff}, the effective dielectric constant, defined by $\epsilon_0 \exp(\alpha_0(r_{ij} - r_0))$ in this particular function, diverges as the distance between charges goes to infinity. For the case when sugar-phosphate backbones are also present, we also used another functional form (Mazur and Jernigan, 1991), Eq. 1 in the preceding article, for V_{es}.

For the calculation of the interrelationships among base-pair coordinates, the conformational states of base pairs are generated in the phase space spanned by the variables twist, roll, tilt, propeller twist, slide, and rise, and the interaction energy is calculated for each conformation. By assuming a canonical distribution in these variables, the partition function and conformational free energy are calculated. For the calculation of the response of conformational coordinates (strain) to the enforced change in one particular coordinate

(stress), the Boltzmann averages of the former coordinates are calculated for each value along the latter coordinate. To take account of longer range interactions and cooperativity among base pairs, we always treat four base pairs or more, and calculations are performed over the sequences of the base pairs iteratively. One base pair at a time is averaged, i.e., the average values of the conformational variables are calculated in succession. After the averages of these variables are computed, one base per each iteration step, the entire process is repeated, until a stationary steady-state solution is obtained. For the calculations of the adiabatic free energy surface, conformational averaging is performed for each value of the base-pair coordinates in the central base step.

The algorithm to determine the conformation of the backbone differs from the method applied to base pairs alone, and the detailed description is given in the preceding article. We take coordinates of the B-form and A-form backbone conformations from crystal structures (Dickerson and Drew, 1981; McCall et al., 1985), and both forms are used as initial structures in the calculations. We have tried other structures as starting structures, but the choice of initial coordinates does not much affect the results described below.

In this paper, we perform computations on tetramer sequences and optimize the backbone conformation, composed of two strands that connect the space-fixed base pairs. Essentially, the two strands are varied independently of one another, because the cross-strand interactions between atoms located in different strands are negligible. The backbone conformational variables considered in the present study are the phosphate torsion angle, sugar pseudorotation phase angle, sugar torsion angle, and the dihedral angle that measures the orientation of the base to the sugar. These phosphate-sugar variables are defined in Saenger's monograph (1984). In the present paper, two tetramer sequences are employed. Those are the GGGG and AAAA sequences. For each of these the base-pair parameters that determine the spatial orientations of the base pairs linked to backbone segments assume identical values in all three steps. Average values of the backbone variables are calculated. To demonstrate the purine-pyrimidine effects on these variables, the averaging is performed separately for each of the two backbone strands. However, to reduce, as much as possible, the undesirable chain-end effects, the computed backbone conformational variables are averaged only over those located in the two interior nucleotide units. The current computations of backbone conformational variables can easily be extended to nonuniform tetramer sequences for any base-pair sequence.

RESULTS

Relationships among conformational variables of base pairs

As mentioned before, conformational variables of base pairs such as slide, twist, and roll vary for different conformations of DNA. Thus, we first examine how these variables are interrelated. At first, we changed slide and examined its effect on twist, roll, and tilt. As described before, the values of twist, roll, and tilt are Boltzmann averaged for each fixed value of slide. The result shows that slide has a strong effect only on the average twist, as shown in Fig. 1; decreasing slide is associated with a decrease in average twist. In this calculation without backbone, we used two sets of electrostatic parameters to mimic different kinds of electrostatic environment. One is the "high screening" case with α_0 of 1.2 $Å^{-1}$ and ϵ_0 of 3; and the other is the "low screening" case with α_0 of 0.5 $Å^{-1}$ and ϵ_0 of 5. In the former case, the long-range electrostatic interactions are screened by solvent and the short-range electrostatic interactions inside the cavity are exaggerated with small ϵ_0; whereas the situation is reversed in the latter case. At "high screening," twist at zero slide is near 40° for the GG/CC step, which is somewhat higher than the average B-form, and varies monotonically to about 25° at −1.5 Å of slide. The change in twist is rather sharp in this slide range, implying a transition-like behavior along the slide coordinate. At "low screening," on the other hand, the change in twist is smaller (from 36° to 27° over the same slide range), but manifests a similar dependence on slide. This effect of slide on twist is caused mainly by the optimization of the stacking interactions between adjacent base pairs, i.e., increasing slide tends to reduce the overlapping surface between adjacent base pairs, which is partly compensated by decreasing twist. Roll and tilt are small and almost constant, regardless of the change in slide. From the crystal structure of d(GGGGCCCC) (McCall et al., 1985), the average values of twist and slide at GG/CC steps ex-

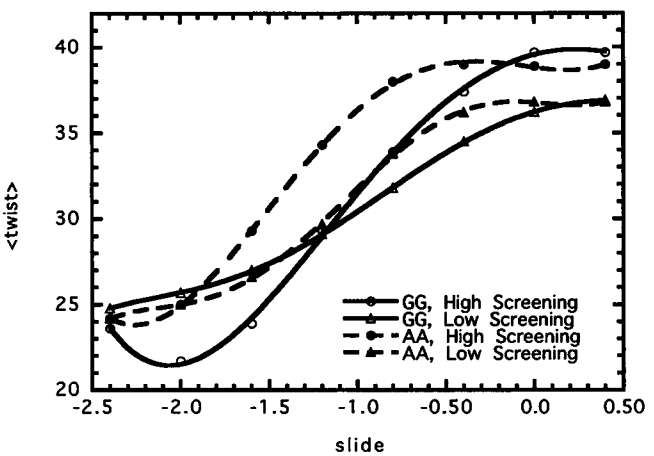

FIGURE 1 Response of ⟨twist⟩ to slide for the GG/CC and AA/TT steps, with "high screening" (○ and ●, respectively) and "low screening" (△ and ▲, respectively) electrostatic environments. Calculations are for the GGGG and AAAA sequences. In this and all other figures and tables, data presented are for the middle pair of base pair steps in a tetramer. This is done to reduce the chain-end effects. All angles are in degrees, and distances in Å. Exponential function (Eq. 1) for the electrostatic energy was used, with α_0 = 1.2 and ϵ_0 = 3 for "high screening," and α_0 = 0.5 and ϵ_0 = 5 for "low screening." For each slide value, Boltzmann averages of twist, roll, and tilt are calculated. The sugar-phosphate backbone is not included in these calculations.

cluding ends are 30.4° and −1.57 Å, respectively, in qualitative agreement with the above results. In the case of the AA/TT step, twist changes from 39° to 30° by decreasing slide from 0 to −1.5 Å at "high screening" (Fig. 1). The effect of screening parameters and insensitivity of roll and tilt to the change in slide are similar in the case of the GG/CC step. We have also analyzed the relation for other sequence steps and find that most of the steps show a similar slide-twist relationship, although CG, AT, and AC/GT steps exhibit a rather flat dependence, indicating a less sharp transition.

On the other hand, forcing twist to change, i.e., twist as the independent fixed variable, causes the average slide to change in a similar manner, but the effect is significantly smaller than the reverse effect of slide on average twist in the case of the GG/CC step, as shown in Fig. 2. The curve is almost flat in the case of the AA/TT step. The twist change causes no significant change to roll and tilt. Likewise, no significant effects of twist on roll or tilt are observed for other sequence steps. Thus, the stress-strain relation is not symmetric between slide and twist when the stress and strain are interchanged, or the driving parameter is changed. Such asymmetries can be anticipated because the effects of the fixed conformation can be smoothly absorbed by average changes to all nonfixed remaining degrees of freedom. Clearly, when one or the other of two variables is fixed, the ways in which the stress is absorbed will be different because different degrees of freedom can change.

In the structure of A-form DNA, base planes are inclined with respect to the global helix axis. The average roll angle at GG/CC steps excluding ends estimated from the direction cosines for the A-form crystal structure of d(GGGGCCCC) (McCall et al., 1985) is 6.3°. The conformational calculations of A-DNA (Mazur et al., 1989) indeed show that roll tends to have positive values in the A-form, with larger magnitude of slide; whereas the average roll is near 0 in the B-form. When the roll angle is increased into the positive range for the GG/CC step, which has a strong tendency to adopt the A-form, Boltzmann-averaged slide decreases and twist decreases to values near those observed in the A-form crystal structure of d(GGGGCCCC) (McCall et al., 1985), as shown in Fig. 3. On the other hand, the change in roll for the AA/TT step, which resists becoming the A-form, does not exert a significant effect on average twist or average slide (Fig. 3). Because changes in slide or twist have little effect on roll, an asymmetrical stress-strain relationship also holds between roll and the other variables. Changing tilt does not affect the other variables significantly, and vice versa.

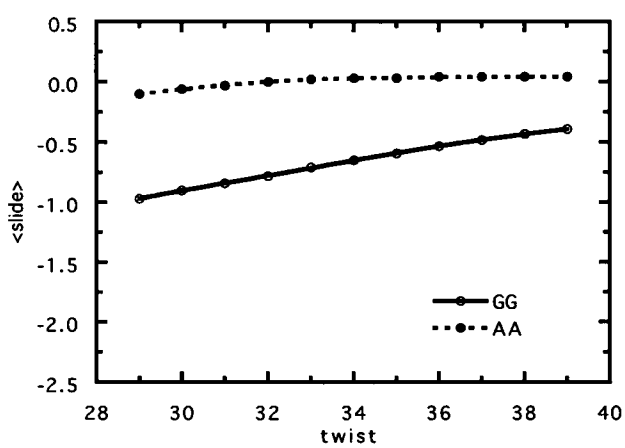

FIGURE 2 Response of ⟨slide⟩ to twist for the GG/CC (○) and AA/TT (●) steps. Other conditions are the same as in Fig. 1.

Effect of twist on the sugar-backbone conformation

We have examined the effect of twist on the backbone conformation by calculating the six backbone torsion angles (α to ζ) and χ, the glycosyl torsion angle. The only torsion angles that show a particularly strong dependence on helical

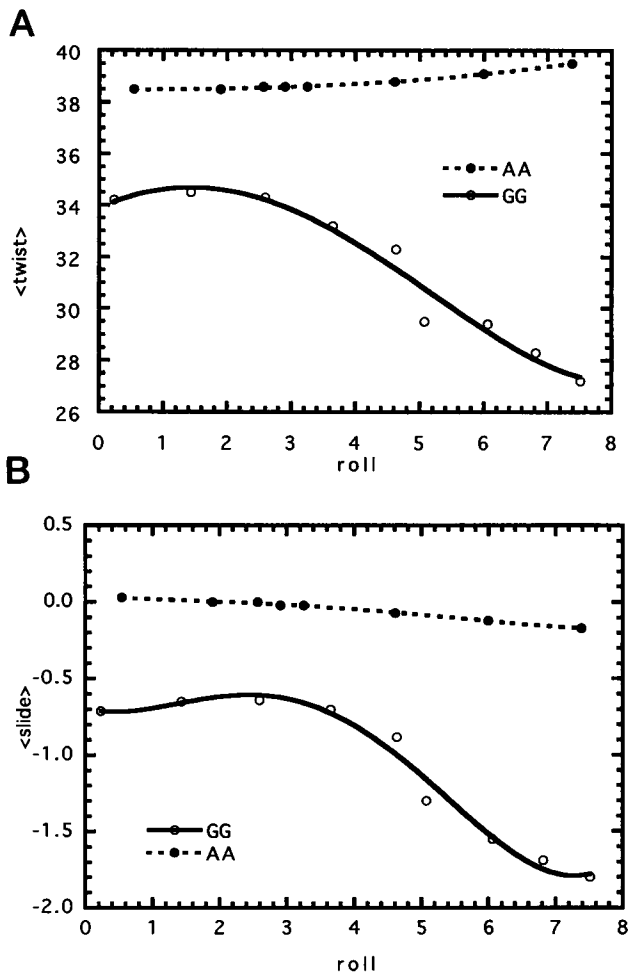

FIGURE 3 Effect of roll on ⟨twist⟩ (*a*) and ⟨slide⟩ (*b*) for GG/CC and AA/TT steps (○ and ●, respectively). Exponential function (Eq. 1) for the electrostatic energy is used, with "high screening" conditions $\alpha_0 = 1.2$ Å^{-1} and $\epsilon_0 = 3$. The sugar-phosphate backbone is not included in these calculations.

twist are δ, defined by $C_{5'}$-$C_{4'}$-$C_{3'}$-$O_{3'}$, and ζ, defined by $C_{3'}$-$O_{3'}$-P-$O_{5'}$. (ν_3, the sugar pucker torsion angle, defined by $C_{2'}$-$C_{3'}$-$C_{4'}$-$O_{4'}$, is often substituted for the torsion angle δ, because both angles describe orientations about the same $C_{4'}$-$C_{3'}$ bond. On average, these two angles differ by 117°.)

Fig. 4 shows the effect of twist on δ and $-\zeta$ with and without lateral translations between adjacent base pairs for the GG/CC step. This figure shows that the torsion angles δ and ζ are always strongly anticorrelated, because they determine the crankshaft rotation about the $C_{3'}$-$O_{3'}$ bond. Because ϵ, the intervening bond, is in the *trans* configuration, the set of the three consecutive torsion angles δ, ϵ, and ζ defines an ϵ crankshaft. If the three consecutive dihedral angles in the crankshaft maintain a *gauche*$^{\pm}$-*trans*-*gauche*$^{\mp}$ arrangement, this crankshaft is designated in the polymer literature as a kink. The nucleotide literature (references quoted in Saenger, 1984) designates as a *gauche*$^+$ a torsion angle in the 30–90° range, *gauche*$^-$ an angle in the 270–330° range, and *trans* an angle in the 150–210° range. In the B-form, the δ and ζ dihedrals are often distorted *gauches*. Those are designated in the nucleotide literature as +anticlinal and −anticlinal angles, respectively. Their indicated ranges are 90–150° and 210–270°, respectively (Saenger, 1984). Fig. 4 indicates that the δ dihedral angle is not a *gauche* but a +anticlinal angle. The ζ dihedral angle can be either a *gauche*$^-$ or a −anticlinal angle.

For twists of 38° and higher (or in the presence of slide for twists of 34° and higher), the ν_3 angle tends to have positive values, which is one of the characteristics of B-DNA. In the case of the dodecamer crystal structure (Dickerson and Drew, 1981), ν_3 is 4.9 ± 17.8°, that is, $\delta \approx 122°$. On the other hand, low twist around 30° causes ν_3 to reach values near −30° ($\delta \approx 87°$). The average ν_3 angle for the A-form crystal, d(GGGGCCCC) (McCall et al., 1985), is −38.9 ± 5.6°. The range of values of ν_3 for overtwisted backbones puts the sugar pucker mode into $C_{2'}$-*endo* range. For undertwisted backbones, ν_3 assumes values that are close to values associated with the sugar pucker in the $C_{3'}$-*endo* mode. The calculated pseudorotation phase angle is about 80°. This puts the sugar pucker mode between the $O_{4'}$-*endo* and $C_{4'}$-*exo* modes. The calculated range in the sugar puckering angle indicates a partial, or incomplete, B-A transition, as the $C_{3'}$-*endo* mode is not yet obtained. We have also examined the effects of a different set of partial atomic charges. For calculations with the larger charges of Weiner et al. (1984) or reduced screening, the transition to the $C_{3'}$-*endo* mode of sugar becomes more complete.

The calculated ζ angle for the overwound GG/CC step (twist in excess of 38°) is between −100° and −110° (Fig. 4). The average value of ζ for the B-form dodecamer crystal structure (Dickerson and Drew, 1981) is −108 ± 34°, in good agreement with the calculated value. On the other hand, the ζ value for the underwound sequences is estimated to be between −70° and −80°, putting this dihedral angle in the gauche$^-$ range. Both the dihedral angles δ (or the endocyclic angle ν_3) and ζ show a sigmoid-like dependence on the amount of helical twist, displaying the existence of two states, each with its own characteristic value. These two states are interconnected by a rather narrow transition region.

We have examined the effect of screening parameters and the differences between purine and pyrimidine strands. Fig. 5 shows the dependence of the sugar dihedral angle and the P-P distance on twist for the GG/CC step. Both strands undergo a transition in δ just before 36°. Changes to δ occur more suddenly than changes to the P-P distance. In the indicated twist range, the pyrimidine sugar pseudorotates to the $O_{4'}$-*exo* mode, whereas the sugar pseudorotation when connected to a purine base stops at the $C_{1'}$-*exo* mode (pseudorotation angle about 126°; see Table 1). The data presented in Tables 1 and 2 confirm the conclusion reached by

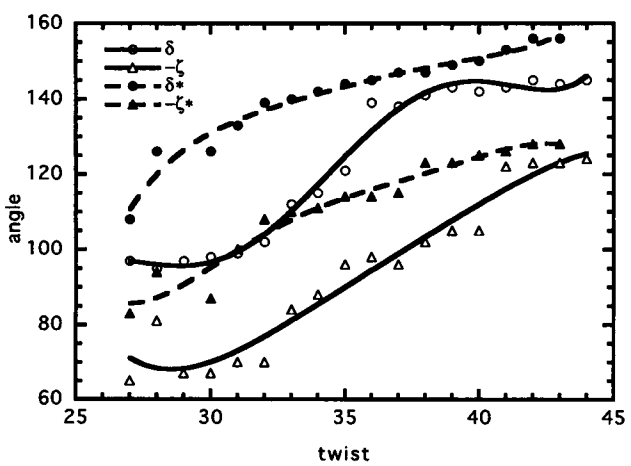

FIGURE 4 Effect of twist on δ and ζ in the absence (○ and △, respectively) and presence (● and ▲, respectively) of slide. In this calculation with backbone structure, the Langevin function (Eq. 2 in the preceding article) for the electrostatic energy is used, with $\kappa_0 = 0.55$ Å^{-1}, $\epsilon_0 = 3$, and r_0 is 4.6 Å. The initial backbone conformation used for the calculation is B-form DNA.

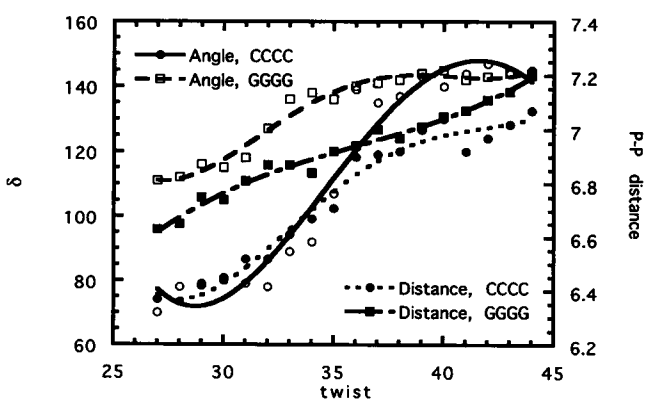

FIGURE 5 Effect of twist on the sugars of pyrimidine and purine strands: δ, ○ and □, respectively; P-P distance, ● and ■, respectively. The Langevin function (Eq. 1 in the preceding article) for the electrostatic energy was used, with $\kappa_0 = 0.55$ and $\epsilon_0 = 3$. Cavity size (r_0) is 4.6 Å. No slide is present.

TABLE 1 Effect of twist on the sugar-backbone morphology for the B-form in the absence of lateral translation between adjacent base pairs

Twist	δ		Pseudorotation		P-P distance	
(°)	CC	GG	CC	GG	CC	GG
28	78	117	68	128	6.36	6.65
30	80	116	69	132	6.45	6.74
32	78	127	52	136	6.52	6.87
34	92	138	83	157	6.67	6.84
36	139	140	167	165	6.90	6.94
38	137	142	170	166	6.92	6.97
40	140	145	175	168	7.04	7.05
42	142	143	171	164	6.97	7.11
44	145	144	171	165	7.07	7.20

Calculations are done for the GGGG sequence. Slide and shift are 0 Å. Langevin function (Eq. 1 in the preceding article) for the electrostatic energy is used, with $\kappa_0 = 0.55$ Å^{-1}, $\epsilon_0 = 3$, and $r_0 = 4.6$ Å. Notice that undertwisting the backbone moves the sugar pucker mode toward its $C_{3'}$-*endo* mode. However, whereas the δ dihedral adopts its A-form value, the pseudorotation stops at the $O_{4'}$-*endo* mode. Therefore, most of the extra stress created by undertwisting the B-form occurs along the phosphate skeleton, with less in the sugar.

Kollman et al. (1982) that pyrimidines are more likely to repucker than purines, which is also in agreement with crystallographic results (Drew et al., 1981). Kollman et al. (1982) also observed that for the overtwisted helices (twist of 40°), all sugars remain in the $C_{2'}$-*endo* pucker mode, whereas for underwound helices (twist of 28°), the sugar tends to assume the $O_{4'}$-*endo* and $C_{3'}$-*endo* modes. The observed difference in the abilities of the purine and pyrimidine connected sugars is strongly correlated to the difference in the electrostatic charge distributions in these bases. The strong electrostatic influence on the abilities of the purine- and the pyrimidine-connected sugars to undergo the $C_{2'}$-*endo*–$O_{4'}$-*exo* mode transition is demonstrated in Tables 1 and 2. In Table 1, data extracted from Fig. 5 are presented. In Table 2, the data based on a weak electrostatic potential field (see footnote for Table 2) are presented. There, with the "low electrostatic screening," both purine- and pyrimidine-connected sugar rings show the same abilities to undergo the $C_{2'}$-*endo*–$O_{4'}$-*exo* mode transition. However, there is still a slight preference for the pyrimidine sugar to undergo this change fully. Generally, the P-P distances follow the same purine-pyrimidine dependence. However, because the backbone skeleton is further removed from the base than is the sugar ring, the purine-pyrimidine effects are not as noticeable there. It should be noted, however, that regardless of the solvent screening action, the P-P distances cannot assume the values that hold in the A-form. The presence of slide (Table 3) strongly suppresses changes to pseudorotation for either purine or pyrimidine sugars. Notice that, for a highly undertwisted backbone (twist of 28°), the presence of lateral translation can create a bistable system.

TABLE 2 Effect of twist on the sugar-backbone morphology for the B-form and "low screening" in the absence of lateral translation between adjacent base pairs

Twist	δ		Pseudorotation		P-P distance	
(°)	CC	GG	CC	GG	CC	GG
28	83	87	82	87	6.42	6.56
30	86	91	83	92	6.53	6.65
32	88	94	81	88	6.62	6.70
34	93	93	84	84	6.73	6.78
36	103	108	99	113	6.86	6.91
38	113	122	99,132	136	6.95	7.03
40	133	140	151	164	7.01	7.05
42	139	143	160	168	7.12	7.14
44	145	147	166	171	7.24	7.25

Calculations are for the GGGG sequence. Slide and shift are 0 Å. In this "low screening" case, exponential function (Eq. 1) is used for the electrostatic energy, with $\alpha_0 = 0.5$ and $\epsilon_0 = 6$. Cavity size (r_0) is 3.0 Å.

It should be remarked that the pseudorotation-twist dependence displays a sigmoid form, indicative of a rapid change to the pseudorotation angle over a narrow range of the twist. This sigmoidal form is seen in Table 1, where the pseudorotation angle changes by more than 100°, whereas the twist changes by a mere 4°. In a "low screening" case (Table 2), a similar sigmoidal form for the pseudorotation angle-twist dependence is displayed, except that the region of the twist that accompanies the rapid change in pseudorotation is now shifted toward larger twist values (from the 32–36° range in Table 1 to the 36–40° range in Table 2). Data presented in these two tables indicate the presence of energy barriers in the pseudorotation cycle. An interpretation of the sigmoid-like pseudorotation-twist dependence, shown in Tables 1 and 2, is that the sugar pucker modes in the B-form of DNA can be in either the $C_{2'}$-*endo* or in the $O_{4'}$-*endo* forms, indicating the presence of a potential bar-

TABLE 3 Effect of twist on the sugar-backbone morphology for the B-form in the presence of lateral translation between adjacent base pairs

Twist	δ		Pseudorotation		P-P distance	
(°)	CC	GG	CC	GG	CC	GG
28	142,94	137	153,108	156	6.81	6.71
30	114	139	128	161	6.72	6.73
32	139	140	161	164	6.74	6.78
34	142	142	163	167	6.87	6.87
36	146	144	166	168	6.97	6.94
38	148	146	165	171	6.97	6.99
40	150	149	168	170	7.07	7.17
42	160	153	178	180	7.71*	7.21

* One *trans* zigzag in β crankshaft (pyrimidine) is present.
Calculations are for the GGGG sequence. Slide is −1.75 Å; shift is −0.5 Å. Other parameters are the same as in Table 1. For a twist of 28°, two different values for δ and pseudorotation angle for pyrimidine-linked sugar are presented, indicating that this particular system is bistable. Note that the presence of translational motions in base pairs hinders the transition of the sugar away from its B-form $C_{2'}$-*endo* mode with backbone undertwisting. However, the total energy (not shown here) shows a stronger increase with decreasing twist when slides are imposed on the backbone than was the case in the absence of slide. Note also that the P-P distances tend to maintain their B-form values over larger ranges of twist in the presence of slides.

rier separating these two sugar pucker modes. Therefore, the emphasis should be on the nature of the pseudorotation-twist dependence, rather than on the particular range of twist values where the pseudorotation angle displays its rapid change. It should be emphasized that only the sugar connected to the pyrimidine base shows the $C_{2'}$-*endo* to the $O_{4'}$-*endo* transition. The purine-connected sugar persists in its $C_{2'}$-*endo* puckering mode, because, in the absence of favorable electrostatic interactions with the five-atom ring unit, the barrier separating the $C_{2'}$-*endo* and the $O_{4'}$-*endo* puckering modes is now considerably higher, and the $O_{4'}$-*endo* mode is not reachable.

The β crankshaft (the three consecutive dihedrals α, β, γ) remains conformationally stable in the B-form over a wide range of twist. This crankshaft maintains its kink-like orientation of *gauche*$^-$-*trans*-*gauche*$^+$. Specifically, $\alpha = -65°$, $\gamma = 60°$ (for no lateral translations), and $\alpha = -72°$, $\gamma = 61°$ (for base pairs with lateral translation). However, in the presence of lateral translations, the kink-like β crankshaft is maintained only over narrower ranges of twist (29°, 40°) than was the case for the straight (no translation) B-form. The reason for this narrower region is that at twists of 40° and higher, the pyrimidine-linked β crankshaft tends to assume an all-*trans* zigzag-like orientation. In the indicated twist range, only one β crankshaft in a base-pair step expands toward a *trans* orientation, whereas the remaining three β crankshafts retained their initial kink-like orientations. Energy considerations dictate that the α, γ dihedral angles be either in *gauche* or in *trans* arrangements. Formation of zigzag-like β crankshafts is necessitated to maintain a low-energy system when the backbone is further stretched; whereas stretching the ϵ crankshaft toward the zigzag-like arrangement is prevented by the inaccessibility of the corresponding sugar puckering mode (the pseudorotation angle then exceeds 180°). It is of interest to notice that it is the pyrimidine-linked backbone segment that undergoes the expansion of the β crankshaft toward the *trans*, zigzag-like orientation. The angle χ, the glycosyl dihedral, is virtually twist-independent, but is strongly correlated with slide (see later).

When the A-form backbone is used as an initial structure, the effect of twist on the backbone dihedral angles is less appropiate for a simple stress-strain analysis, because of the relative inflexibility of the backbone. Response of the A-form backbone to changes in twist is no longer elastic, because the ϵ crankshaft cannot be easily deformed, and because of the restrictions imposed by the sugar pseudorotation. The β crankshaft shows the same abrupt kink-zigzag transition that was already noticed for the highly overtwisted backbone segments in their B-form when slides are present. In other words, the α and γ dihedrals are in either one of the two *gauche* orientations or in the *trans* orientation, as long as the β dihedral angle maintains its near-*trans* arrangement. Table 4 shows the effect of twist on the backbone dihedral angles when the A-form backbone was used for the initial structure. The calculated values of ζ shown in this table are in good agreement with the average value of ζ for the A-form crystal, d(GGGGCCCC) (McCall et al., 1985), of $-70 \pm 10°$. The average value for ζ in the indicated range of twist is $-74°$. Thus, the calculated ζ angles for B- and A-form conformations show semiquantitative agreement with those observed in crystal structures. Table 4 shows that for the A-form, the ϵ crankshaft, the values of the angles δ and ζ, is virtually independent of twist. This is in contrast with the results obtained for the calculation starting from the B-form conformation, which shows a gradual tendency of this crankshaft to assume a more *trans*, zigzag-like orientation. All of the dihedral angles in this crankshaft, that is, δ, ϵ, ζ, tend toward all-*trans* orientations.

The ϵ crankshaft assumes its stable arrangement of *gauche*$^-$-*trans*-*gauche*$^+$, referred to as a kink, which is known to be conformationally stable and, therefore, not susceptible to steric deformation. Therefore, the terminal dihedral angles in the ϵ crankshaft are *gauche*$^+$ and *gauche*$^-$ in the A-form, and +anticlinal and −anticlinal in the B-form. When the A-form is subjected to large stresses and forcibly overtwisted, the most likely configurational changes occur primarily in the β crankshaft. Table 4 shows that, for undertwisted backbones, which are typical of the

TABLE 4 Effect of twist on the backbone dihedral angles for the A-form

Twist (°)	α	β	γ	δ	ϵ	ζ	χ	Energy
30	−67	164	65	78	−173	−72	−157	−21.8
31	−72	165	63	79	−172	−73	−159	−17.4
32	−74	165	66	80	−169	−72	−161	−17.7
33	−75	164	68	77	−166	−71	−163	−18.1
34	−73	164	67	77	−167	−70	−164	−20.4
35	—	168	65	81	−173	−76	−162	−26.7
36	—	168	65	79	−170	−73	−164	−24.2
37	—	168	64	83	−172	−76	−164	−24.7
38	—	177	—	82	−170	−75	−167	−29.9
39	—	178	—	84	−170	−76	−169	−28.0
40	—	176	—	84	−169	−78	−171	−25.3

The A-form backbone was used for the initial structure. Data are for the GGGG sequence. Slide = 1.5 Å and shift = 0.0. Langevin function (Eq. 1 in the preceding article) for the electrostatic energy is used, with $\kappa_0 = 0.55$ Å^{-1}, $\epsilon_0 = 3$, and $r_0 = 4.6$ Å. All angles here are averages taken over all four dihedrals in the centrally located base pair step. No value given indicates that one or more of the indicated dihedral angles are in a *trans*-like orientation; the data are given separately in Table 5.

A-form, the changes in the β crankshaft are small and gradual, with most of the changes confined to the α dihedral angle. For twists of 35° and higher, the changes are abrupt. Table 5 shows, in more detail, how the two dihedrals in the β crankshaft respond to a gradual increase in the amount of twist for the range of 35° and higher. This table shows that these angles jump from the initial *gauche* to the final *trans* arrangement, without values in the intermediate anticlinal ranges. For moderately overtwisted backbones (twist in the range (35°, 37°), only one of the two pyrimidine-linked α dihedrals assumes a *trans* orientation. If the twist exceeds 38°, both pyrimidine-linked α dihedral angles jump to the straight *trans* 180°. Simultaneously, one of the pyrimidine-linked γ dihedrals assumes a near-*trans* value. The inability of the γ dihedral to assume the completely *trans* orientation of 180° is presumably due to its proximity to the sugar ring. Data presented in Table 5 are for twists in the 35°, 42° range. For twists exceeding 42°, purine-connected α and γ dihedrals undergo this *gauche*-to-*trans* transition, "one at time," until, for sufficiently large twists, all β crankshafts can assume zigzag-like arrangements. Table 4 also shows the total energy of the system. This is shown to demonstrate that the *gauche-trans* transitions in the β crankshafts do maintain low energies in the A-form under overtwisting stress.

It is known that the GG/CC step is more likely to assume the A-form than is the AA/TT step. It is of interest, therefore, to examine the behavior of the AA/TT step in the A-form when it is subject to increasing twist. Our calculations show that, as expected, the β crankshaft reaches its *trans*, zigzag-like orientation more readily in the AA/TT step than in the GG/CC step. Specifically, the AA/TT step also displays a partial zigzag β crankshaft in purine when twist exceeds 42°.

Figs. 6 and 7 present the response in energy to the stress exerted by the change in twist. When lateral translations between adjacent base pairs are absent, the total energy is seen to decrease with increased twist (Fig. 6). The increase in energy occurs primarily at twists below 32°. The AA/TT step displays a sharper increase in the total energy when undertwisted than is the case with the GG/CC steps. When lateral translations are present, the total energy is always higher than in the absence of translations. Moreover, in the indicated twist range (25° to 45°), the total energy with lateral translation has a minimum value at twist ≈ 35° for AA/TT and at ~40° for GG/CC. When the total energy is decomposed into van der Waals and electrostatic components, the van der Waals terms display a minimum at twist ≈ 36° in the presence of lateral translations for both GG/CC and AA/TT steps. The presence of lateral translations usually leads to an increase in the van der Waals energy because of increased dispersion energies due to

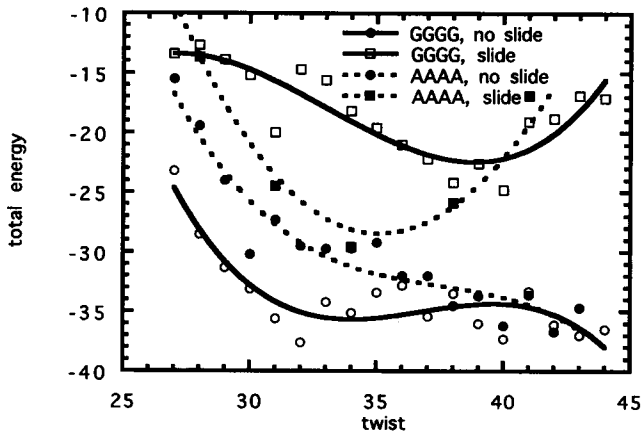

FIGURE 6 Effect of twist on the total energy for an A-form backbone. The initial backbone conformation used for the calculation is A-form DNA. Calculations are done for the GGGG and AAAA with slide (−1.5 Å; □ and ■, respectively) and without slide (○ and ●, respectively). Langevin function (Eq. 1 in the preceding article) for the electrostatic energy is used, with $\kappa_0 = 0.55$ and $\epsilon_0 = 3$. Cavity size (r_0) is 4.6 Å.

TABLE 5 Effect of twist on α and γ of purine and pyrimidine strands for the A-form

Twist	Pyrimidine		Purine	
(°)	α	γ	α	γ
35	−78,180	65	−73	66
36	−78,180	65	−73	70
37	−68,−175	64	−76	70
38	−177	64,146	−76	71
39	−178	66,150	−79	71
40	179	71,151	−77	70
41	180	66,148	−83	70
42	180	73,140	−79	73

The same as in Table 4, but only for the twist range where more than one stable dihedral angle is indicated. Whenever a single angle value appears in any column, it represents an average value over two adjoining dihedrals in the given strand. Otherwise, both dihedrals are presented. Average values are presented whenever individual angles differ by less than 5°. This table lists only the cases when one or more dihedrals in the β crankshaft have a zigzag-like orientation.

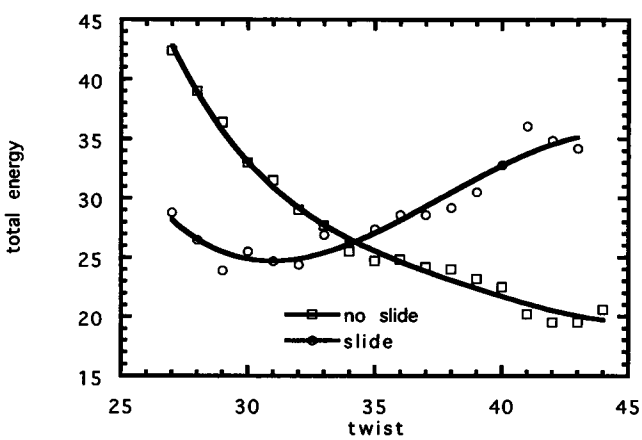

FIGURE 7 Effect of twist on the total energy for B-form backbone with "low screening." Calculations are done for the GGGG with slide (−1.5 Å) and without slide (○ and □, respectively). In this "low screening" case, exponential function (Eq. 1) was used for the electrostatic energy, with $\alpha_0 = 0.5$ and $\epsilon_0 = 6$. Cavity size (r_0) is 4.6 Å.

larger distances between the backbone atoms of adjoining nucleotides. Therefore, the changes in the total energy that accompany backbone twisting are primarily attributed to the accompanying changes in the van der Waals (primarily dispersion) forces. This scenario changes when lateral translations are present. The additional separation between nearest charges brought by lateral displacements between adjoining base pairs tends to further energetically destabilize the undertwisted double helices.

The situation changes for the "low screening" case. The stress-strain relation in the B-form involves the lateral base pair translation in addition to the helicity. This is demonstrated in Fig. 7. Here, the calculations presented in Fig. 6 are repeated with "low screening." Fig. 7 shows the total energy versus twist for the GG/CC step, with and without lateral translation. The result shows that the presence of lateral translations lowers the energy for the undertwisted backbones (twist of less than 34°). The van der Waals energy component shows a similar trend. This stabilizing effect of lateral translations on the energy of the undertwisted sequences was absent in the highly screened dielectric systems (Fig. 6). Therefore, for low dielectric screening in the extended twist range shown in Fig. 7, the stress-strain relation must involve lateral translations of the base pairs as well as base-pair rotations about their local helix axes.

Effect of slide on sugar-backbone conformation

So far, we have used only twist as the extensive variable in the stress-strain examination of the conformational variables of the A- and B-forms of DNA. We have also examined the effect of variable slide on the backbone conformation by calculating backbone dihedral angles as functions of slide. The change in slide does not cause large or drastic changes in the backbone dihedral angles. The only angle exhibiting a substantial range of variation is χ, the glycosyl bond rotation about the bond that links the sugar to the base. Fig. 8 shows the dependence of χ on slide for the A- and B-forms of DNA. The calculations are performed for a twist angle of 30°. As shown in this figure, slide and χ are strongly correlated in both B- and A-forms of DNA. However, the range of χ dihedral angles for the (0, −1.5 Å) range of slides is narrower (20°) for the A-form than for the B-form (32°).

At zero slide, the calculated value of χ for the B-form is −118° (see Fig. 8), which is very close to the average value of χ (−117°) observed in the B-form dodecamer crystal structure (Dickerson and Drew, 1981). The decrease of slide to −1.5 Å causes the value of this angle to decrease to −150°. Notice that for slides of less than −0.75 Å, χ adopts values associated with the A-form, even though the sugar pucker mode is the one characteristic of the B-form. On the other hand, the dihedral angle χ shows a somewhat smaller decrease with slide for the A-form (Fig. 8). The χ angle for the A-form crystal, d(GGGGCCCC) (McCall et al., 1985), is −158 ± 10°. Thus, the response of χ to slide is consistent with structural observations of the A- and B-forms.

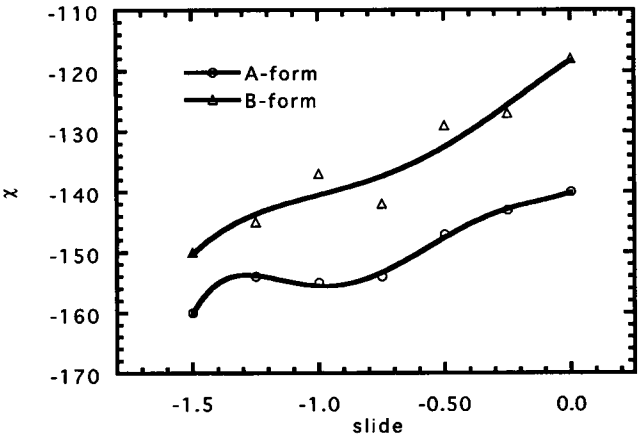

FIGURE 8 Effect of slide on χ. Shift is −0.5 Å. Calculations are for the GGGG sequence with B-form (upper curve) and A-form (lower curve) as the starting backbone conformation. Twist angle is 30°. Langevin function (Eq. 1 in the preceding article) for the electrostatic energy is used, with κ_0 = 0.55 Å^{-1}, ϵ_0 = 3, and r_0 = 4.6 Å.

We also have investigated the roles of variable amounts of roll and tilt angles, within their experimentally observed ranges, in the conformational variables of the backbone, and in the P-P distances and pseudorotation angles. The effects of these variables are found to be rather insignificant.

DISCUSSION

The present stress-strain analyses show that the conformational variables describing base-pair geometry (twist, roll, tilt, slide, shift) and backbone morphology are strongly correlated with each other. The calculations for base pairs show that slide, twist, and roll are correlated in a manner consistent with experimental observations on the structures of DNA in the B- and A-forms. On the other hand, the results also show that the stress-strain relationships are not symmetrical with respect to these variables: enforcing a change in slide affects average twist much more than a change in twist affects average slide. Likewise, the effect of a change in roll on average slide and average twist is larger than in the other direction. These stress-strain relations are sequence dependent. Such asymmetrical stress-strain relations reflect the nonuniform structure of DNA, particularly in terms of which stresses exert strain more effectively than others. The asymmetries in stress-strain relationships are more evident when the direction of the B-A transition is reversed, that is, when the same changes in twist and slide in an opposite direction are enforced on both forms of the backbone conformations. One of the reasons for the apparent irreversibility of the B-to-A transition is that the energy considerations force the A-form not toward the B-form but toward an extended, low-energy backbone segment with a zigzag-like β crankshaft, while simultaneously preserving the initial sugar pucker mode. Therefore, in the present discussion, the term "B-A transition" is applied solely to the conformational changes to the B-form of the DNA.

The effects of conformational changes of base pairs on the sugar-backbone structure are also different from one variable to another. The change in twist can cause a conformational transition of the sugar between $C_{2'}$-*endo* and $C_{3'}$-*endo*, which is one of the most characteristic conformational aspects of the B-A transition. It also affects the ζ dihedral angle. On the other hand, the only significant effect of slide on angles is exerted on the glycosyl torsion angle χ. Roll and tilt cause less pronounced effects on particular backbone conformations. Thus, the present calculations suggest that twist is the most effective conformational coordinate of base pairs in affecting the sugar-backbone conformation. In the reverse transition, a change in twist does not rotate the sugar from its $C_{3'}$-*endo* mode, nor does it affect the ζ dihedral angle. Instead, changing twist rotates the β crankshaft from a *gauche*$^-$-*trans*-*gauche*$^+$ configuration toward a zigzag (*trans, trans, trans*) configuration. On the other hand, the slide-χ correlation is independent of the direction of the transition.

Slide and sugar pucker are two of the main characteristics of the B- and A-forms. Experimental analyses have shown that base sequence affects the preference for slide (Shakked and Kennard, 1985), e.g., poly(dG)-poly(dC) favors larger slide, whereas poly(dA)-poly(dT) favors smaller slide and resists taking the A-form. Calladine and Drew (1984) concluded from statistical analysis of A-DNA structures that certain kinds of base-pair steps show bistable characteristics, segregated in their slide-roll values. The previous conformational analyses have shown that slide preference is also dependent on the dielectric environment in a sequence-specific manner (Mazur et al., 1989). This effect can be partially attributed to the screening of electrostatic interactions by high dielectric water and hydrated ions, because the electrostatic component of the total nonbonded energy favors the A-form over the B-form, whereas the van der Waals component favors the B-form over the A-form (Mazur et al., 1989). The hydration around base pairs may also affect slide preferences (Drew and Dickerson, 1981; Calladine and Drew, 1984). Considering these circumstances, slide should play an important role in the B-A transition by sensing the sequence and environmental changes directly. However, the present analysis shows that slide does not affect sugar puckering directly, but rather it is the twist that affects the sugar puckering more. On the other hand, the present stress-strain analysis shows that changing slide causes twist to respond. Thus, we arrive at the following pathway for the B-to-A transition: changing dielectric environment or water activity around base pairs may cause base pairs to slide along the long axis of the base pair to adjust their exposure to solvent, i.e., their stacking may change. Because of little resistance from the backbone, this, in turn, unwinds base pairs about the helix axis at the same time. This change in twist causes repuckering of sugar rings from the $C_{2'}$-*endo* to the $C_{3'}$-*endo* forms. It also causes other backbone conformational variables such as the ζ dihedral angle to change. These changes are all associated with changes in other characteristics such as groove widths and P-P distances.

The present analyses also show that roll can drive twist and slide for some sequences, i.e., increasing roll tends to decrease slide and twist. This is consistent with the roll-slide and roll-twist correlations found by analyses of A- and B-DNA crystal structures (Calladine and Drew, 1984; Gorin et al., 1995). The present result suggests that external bending stress can cause some sequences to adopt the A-form. Furthermore, changes in environmental effects on the backbone such as hydration around phosphate groups (Saenger et al., 1986) can drive the B-A transition. Tung (1992) has shown, by Monte Carlo calculations, that the B-A transition can be induced by forcing the pseudorotation angle from $C_{2'}$-*endo* to $C_{3'}$-*endo*, and that slide does not drive the transition. However, it is not so clear how an environmental change or sequence change can force the pseudorotation of sugar directly. The present analyses have shown that slide does not affect the sugar conformation directly, but can affect it indirectly by changing twist, which in turn has a strong effect on the sugar conformation. The fact that slide is more sensitive to the dielectric environment and the base sequence compared to other conformational variables indicates that slide is likely to serve as a key reaction coordinate for the B-A transition. Slide could sense the environmental and sequence differences and respond in a direct way to cause other conformational variables to respond and to move in lockstep. The transition-like behavior associated with the slide coordinate is thus consistent with the idea that the sliding motion along the base pair's long axis can function as a switch between the B- and A-forms (Calladine and Drew, 1984). In our previous conformational analyses of DNA, it was shown that the conformation of DNA and its sequence dependence are mostly determined by the specific interactions between adjacent base pairs, and that the backbone segments play a substantially passive role in determining the conformation (Sarai et al., 1988b). The electrostatic interactions between partial atomic charges on adjacent base pairs play a major role in determining the specific stacking geometries of base pairs and their changes upon environmental and sequence changes. The present results suggest that the direct interactions between base pairs not only determine preferred stacking forms but also play an important role in the overall conformation transitions of DNA.

In our previous conformational analyses of base-pair morphology without backbone (Sarai et al., 1988b, 1989; Mazur et al., 1989), we parameterized the electrostatic interactions so that the calculated structure best reproduced the experimentally observed structure. In the calculations here, which include the backbone structure, however, the same parameterization cannot apply, because the previous calculations included the effects of ions and backbone only implicitly in a potential of mean force through the parameter values. In fact, we have found that it is necessary to increase the cavity size considerably (to around 4.6 Å) to obtain the observed backbone conformation of the A-form. Thus, the adopted cavity size is large enough to incorporate the

charges of a base located near the glycosyl junction. This increased cavity size enhances the differential effect between purine and pyrimidine on the backbone geometry. The larger cavity size may also reflect the effects of ions and hydration around DNA. Saenger et al. (1986) observed structured waters between adjacent phosphate groups in the crystal structures of A-DNA. The larger cavity size may include the structured waters around DNA, making the DNA surface thus less susceptible to the effects of bulk water.

The present type of calculation in which one conformational variable is fixed and all others are averaged is useful for probing conformational coordinates independently in response to environmental and sequence changes, and for finding the important interrelationships among various conformational variables. A similar approach was adopted by Srinivasan and Olson (1987). In their work, the glycosyl (χ) and two sugar torsion angles (pseudorotation angle and δ sugar dihedral angle) are treated as independent variables. In the Srinivasan-Olson methodology, it is the $O_{3'}$-$O_{5'}$ distance that is used as the closure determinant. In our present modeling, it is the P-$O_{3'}$ distance that serves this purpose (see the preceding paper). Conformational calculations of DNA are typically complicated by the presence of large numbers of conformers with similar energies. The thermodynamic averaging over other conformational variables as performed here is of critical importance to smoothing the effects of other degrees of freedom. Otherwise, large numbers of local minima would usually obscure overall features. Furthermore, this type of calculation is useful in interpreting the environmental and sequence dependences of conformational transitions in terms of the chemical structure of the molecule. The present results that indicate the most important conformational parameters could be utilized to suggest directly sets of experiments to modify chemically the bases, either to facilitate or to inhibit these transitions. Chemical substituents could be added to bases in specific ways to modify the atomic charges of strongly interacting atoms, or to block physically motions in some direction, and hence prohibit or enhance their conformational transitions.

Computations were performed on the Cray Y-MP at the Frederick Biomedical Super Computing Laboratory, Frederick, MD.

This research was partly supported by the National Cancer Institute, Department of Health and Human Servies, under contract with SAIC. The content of this article does not necessarily reflect the views of the Department of Health and Human Services, nor does mention of trade names, commercial products, or organizations imply endorsement by the U.S. government.

REFERENCES

Alden, C. J., and S.-H. Kim. 1979. Solvent-accessible surfaces of nucleic acids. *J. Mol. Biol.* 132:411–434.

Arnott, S., and D. W. L. Hukins. 1972. Optimised parameters for A-DNA and B-DNA Biochem. *Biophys. Res. Commun.* 47:1504–1510.

Arnott, S., and E. Selsing. 1974. The structure of polydeoxyguanylic acid with polydeoxycytidylic acid. *J. Mol. Biol.* 88:551–552.

Bloomfield, V. A., D. Crothers, and I. Tinoco. 1974. Physical Chemistry of Nucleic Acids. Harper and Row, New York.

Briki, F., and D. Genet. 1994. Canonical analysis of correlated atomic motions in DNA from molecular dynamics simulation. *Biophys. Chem.* 52:35–43.

Calladine, C. R., and H. R. Drew. 1984. A base-centered explanation of the B-A transition in DNA. *J. Mol. Biol.* 178:773–782.

Dickerson, R. E., M. Bansal, C. R. Calladine, S. Diekmann, W. N. Hunter, O. Kennard, E. von Kitzing, R. Lavery, H. C. M. Nelson, W. K. Olson, W. Saenger, Z. Shakked, H. Sklenar, D. M. Soumpasis, C.-S. Tung, A. H.-J. Wang, and V. B. Zhurkin. 1989. Definitions and nomenclature of nucleic acid structure parameters, *EMBO J.* 8:1–4.

Dickerson, R. E., and H. R. Drew. 1981. Structure of a B-DNA dodecamer. II. Influence of base sequence on helix structure. *J. Mol. Biol.* 149: 761–786.

Drew, H. R., and R. E. Dickerson. 1981. Structure of a B-DNA dodecamer. III. Geometry of hydration. *J. Mol. Biol.* 151:535–556.

Drew, H. R., R. M. Wing, T. Takano, C. Broka, S. Tanaka, K. Itakura, and R. E. Dickerson. 1981. Structure of a B-DNA dodecamer: conformation and dynamics. *Proc. Natl. Acad. Sci. USA.* 78:2179–2183.

Fritsch, V., G. Ravishanker, D. L. Beveridge, and E. Westhof. 1993. Molecular dynamics simulations of poly(dA)·poly(dT): comparisons between implicit and explicit solvent representations. *Biopolymers.* 33: 1537–1552.

Goldstein, H. 1981. Classical Mechanics. Addison-Wesley Publishing Company, New York.

Gorin, A. A., V. B. Zhurkin, W. K. Olson. 1995. B-DNA Twisting correlates with base-pair morphology. *J. Mol. Biol.* 247:34–48.

Ivanov, V. I., L. E. Minchenkova, A. K. Schyolkina, and A. L. Poletayev. 1973. Different conformations of double-stranded nucleic acid in solution as revealed by circular dichroism. *Biopolymers.* 12:89–100.

Kollman, P., J. W. Keepers, and P. Weiner. 1982. Molecular-mechanical studies on d(CGCGAATTCGCG)2 and dA12·dT12: an illustration of the coupling between sugar repuckering and DNA twisting. *Biopolymers.* 21:2345–2376.

Lavery, L. 1988. Junctions and bends in nucleic acids: a new theoretical modeling approach. *In* Structure and Expression. Vol. 3: DNA Bending and Curvature. W. K. Olson, M. H. Sarma, R. Sarma, and M. Sundaralingam, editors. Adenine Press, New York. 191–211.

Leslie, A. G. W., S. Arnott, R. Chandrasekaran, and R. L. Ratliff. 1980. Polymorphism of DNA double helices. *J. Mol. Biol.* 143:49–72.

Levitt, M., and A. Warshel. 1978. Extreme conformational flexibility of the furanose ring in DNA and RNA. *J. Am. Chem. Soc.* 100:2607–2613.

Mazur, J., and R. L. Jernigan. 1991. Distance-dependent dielectric constants and their application to double-helical DNA. *Biopolymers.* 31: 1615–1629.

Mazur, J., A. Sarai, and R. L. Jernigan. 1989. Sequence dependence of the B-A conformational transition of DNA. *Biopolymers.* 28:1223–1233.

McCall, M., T. Brown, and O. Kennard. 1985. The crystal structure of d(G-G-G-G-C-C-C-C). A model for poly(dG)-poly(dC). *J. Mol. Biol.* 183:385–396.

Olson, W. K., and P. J. Flory. 1972. Spatial configuration of polynucleotide chains. II. Conformational energies and the average dimensions of polyribonucleotides. *Biopolymers.* 11:25–56.

Pilet, J., and J. Brahms. 1972. Dependence of B-A conformational change in DNA on base composition. *Nature New Biol.* 236:99–100.

Pohl, F. M., and T. M. Jovin. 1972. Salt-induced co-operative conformational change of a synthetic DNA: equilibrium and kinetic studies with poly(dG-dC). *J. Mol. Biol.* 67:375–396.

Saenger, W. 1984. Principles of Nucleic Acid Structure. Springer-Verlag, New York.

Saenger, W., W. N. Hunter, and O. Kennard. 1986. DNA conformation is determined by economics in the hydration of phosphate groups. *Nature.* 324:385–388.

Sarai, A., J. Mazur, R. Nussinov, and R. L. Jernigan. 1988a. Sequence dependence of DNA conformations: means and fluctuations. *In* Structure and Expressions, Vol. 3. W. K. Olson, M. H. Sarma, and M. Sundaralingam, editors. Adenine Press, New York. 213–222.

Sarai, A., J. Mazur, R. Nussinov, and R. L. Jernigan. 1988b. Origin of DNA helical structure and its sequence dependence. *Biochemistry.* 27: 8498–8502.

Sarai, A., J. Mazur, R. Nussinov, and R. L. Jernigan. 1989. Sequence dependence of DNA conformational flexibility. *Biochemistry.* 28: 7842–7849.

Sarma, M. H., G. Gupta, and R. H. Sarma. 1986. 500-mHz 1H NMR study of poly(dG)-poly(dC) in solution using one-dimensional nuclear Overhauser effect. *Biochemistry.* 25:3659–3665.

Sasisekharan, V. 1973. Conformation of polynucleotides. *Jerus. Symp. Quantum Chem. Biochem.* 5:247–260.

Shakked, Z., and O. Kennard. 1985. The A-form of DNA. *In* Biological Macromolecules and Assemblies, Vol. 2. A. McPherson and F. Jurnak, editors. Wiley, New York. 1–36.

Srinivasan, A. R., and W. K. Olson. 1987. Nucleic acid model building: the multiple backbone solutions associated with a given base morphology J. *Biomol. Struct. Dyn.* 4:895–938.

Tung, C.-S. 1992. A reduced set of coordinates for modeling DNA structures: (I) A B-A transition pathway driven by pseudorotation angle. *J. Biomol. Struct. Dyn.* 6:1185–1194.

Tung, C.-S. and S. C. Harvey. 1986. Computer graphics program to reveal the dependence of the gross three-dimensional structure of the B-DNA double helix on primary structure. *Nucleic Acids Res.* 14:381–387.

Ulyanov, N. B. and V. B. Zhurkin. 1985. Anisotropic flexibility of DNA depends upon base sequence. Conformational calculations of double-stranded tetranucleotides. *Mol. Biol. (USSR).* 18:1366–1384.

Weiner, S. J., P. A. Kollman, D. A. Case, J. C. Singh, C. Ghio, G. Alagona, S. Profeta, and P. J. Weiner. 1984. A new force field for molecular mechanical simulation of nucleic acids and proteins. *J. Am. Chem. Soc.* 106:765–784.

Zhurkin, V. B., Y. P. Lysov, V. I. Ivanov. 1978. Different families of double-strand conformations of DNA as revealed by computer calculations. *Biopolymers.* 17:377–412.

Zhurkin, V. B., V. I. Poltev, and V. I. Florent'ev. 1981. Atom-atom potential functions for conformational calculations of nucleic acids. *Mol. Biol.* 14:887–895.